Int. J. Solids Structures, 1977, Vol. 13, pp. 1281–1291. Pergamon Press. Printed in Great Britain

CAUSTICS CREATED FROM SIMPLY SUPPORTED PLATES UNDER UNIFORM LOADING

P. S. THEOCARIS

Department of Theoretical and Applied Mechanics, The National Technical University, Athens 625, Greece

(*Received* 18 *January* 1977; *Revised* 2 *May* 1977)

Abstract—The method of caustics is applied to problems of simply supported plates under uniform loading. The shape and properties of the *caustic*, created by an initial curve lying inside the plate, as well as the *pseudocaustic* created by the edges of the plate, are completely investigated. It is shown that it is possible to determine the existing loading of the plate from the experimentally determined caustic or pseudocaustic. The cases of simply supported circular, triangular and square plates subjected to uniform loading are examined in detail. It is shown that the experimentally obtained caustics are in good agreement with their corresponding theoretical forms, indicating thus the accuracy of the method of caustics to the study of flexed plate problems.

1. INTRODUCTION

The method of caustics, introduced by Theocaris[1] and successfully applied to a series of singular stress fields in elastic and plastic media[2–5], was then used for the experimental solution of flexed plate problems[6]. The advantages of this experimental technique over most well-known techniques for the experimental solution of flexed plate problems were emphasized. The cases of a triangular plate loaded by a uniform moment distribution along its edges, as well as the problem of the axisymmetric plates were considered as examples to show the potentialities of the method. However, in Ref. [6] only one case of plate and loading was possible to be solved.

In this paper, the theory of Ref. [6] will be generalized and extended to incorporate the caustics and pseudocaustics created by uniformly loaded plates. The cases of circular, equilateral triangular and square plates will be treated in detail. It is shown that the theoretical forms of the caustics and pseudocaustics created by such plates are in good agreement with the experimentally obtained caustics and pseudocaustics. It was concluded that the method of caustics can be successfully used for the experimental determination of the existing loading on plates, in the same way as it has been already used for the analogous problems of elastic and plastic media under generalized plane stress conditions.

2. THE METHOD OF CAUSTICS

In accordance with the method of caustics, a correspondence between each point $P(x, y)$ of the plate and its reflected image $P'(u, v)$ on a reference screen is established (Fig. 1). It was shown that, if $w(x, y)$ is the deflection of the plate, obeying the differential equation [7, p. 82]:

$$\Delta^2 w(x, y) = q/D, \tag{1}$$

where $q = q(x, y)$ is the normal loading and D the flexural rigidity of the plate, it is valid that[6]:

$$u = \lambda\left(x + \frac{2z_0}{\lambda}\frac{\partial w}{\partial x}\right), \quad v = \lambda\left(y + \frac{2z_0}{\lambda}\frac{\partial w}{\partial y}\right). \tag{2}$$

In eqns (2), z_0 is the distance between the screen and the plate, considered as positive, and λ is the magnification ratio of the optical arrangement given by:

$$\lambda = (z_0 + z_i)/z_i\ , \tag{3}$$

where z_i is the distance between the focus of the convergent or divergent light beam impinging

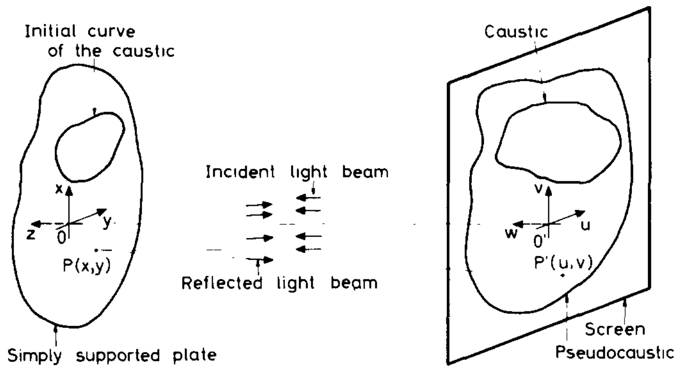

Fig. 1. Geometry of a plate illuminated by a parallel light beam and relative position of the plate and the screen where the pseudocaustic and the caustic are formed.

on the specimen and the specimen itself. Through eqns (2), a correspondence between the points $P(x, y)$ of the plate and $P'(u, v)$ of the screen is established.

If we consider the boundary of the plate expressed in a parametric form: $x = x(s)$, $y = y(s)$ (e.g. as a function of the arc-length s along it), then a corresponding curve is determined on the screen, through eqns (2), which is a boundary of the image of the plate on the screen. This curve, called *pseudocaustic*, is generated by the image of the boundary of the plate. Its parametric equations are functions of the parameter s used for the parametric expression of the boundary of the plate.

It can also be shown that, besides the pseudocaustic, related to the real boundary of the plate, another characteristic curve on the screen, called *caustic*, is formed. The caustic has the property that the points of the plate in the neighbourhood of the points corresponding to the points of the caustic have their corresponding images on the screen lying always in the same side of the caustic. Thus, the caustic can be defined as the curve limiting the points $P'(u, v)$ on the screen, determined by eqns (2), or the curve formed by the relative maxima or minima of u and v, under the constraints $v = \text{constant}$ and $u = \text{constant}$ respectively. In the one side of the caustic a high density of light rays reflected from the plate is observed.

For the creation of a caustic on the screen, a necessary, but not sufficient, condition is that the points $P(x, y)$ on the plate and the corresponding points $P'(u, v)$ on the screen fulfill the condition[1, 6]:

$$J = \frac{\partial(u, v)}{\partial(x, y)} = \begin{vmatrix} \dfrac{\partial u}{\partial x} & \dfrac{\partial u}{\partial y} \\ \dfrac{\partial v}{\partial x} & \dfrac{\partial v}{\partial y} \end{vmatrix} = 0, \tag{4}$$

that is they cause the zeroing of the Jacobian determinant J of (u, v) with respect to (x, y). Then the points $P'(u, v)$ in the neighbourhood of the points of the caustic (and only in the one side of it) do not correspond in only one way to the corresponding points $P(x, y)$ of the plate. Equation (4) defines on the plate a curve from which the caustic on the screen is created. This curve is called the *initial curve* of the caustic.

In the sequel, we will study the caustics formed from simply supported plates under uniform loading q and namely the cases of circular, equilateral triangular and square plates. Before proceeding to these problems, we can also observe that eqn (4) for the initial curve of a caustic can also be written, because of eqns (2), under the form:

$$J = \begin{vmatrix} 1 + \dfrac{2z_0}{\lambda}\dfrac{\partial^2 w}{\partial x^2} & \dfrac{2z_0}{\lambda}\dfrac{\partial^2 w}{\partial x \partial y} \\ \dfrac{2z_0}{\lambda}\dfrac{\partial^2 w}{\partial x \partial y} & 1 + \dfrac{2z_0}{\lambda}\dfrac{\partial^2 w}{\partial y^2} \end{vmatrix} = 0. \tag{5}$$

If the function w is expressed in polar coordinates (r, ϑ), that is $w = w(r, \vartheta)$, then eqns (2) and (4) of the caustic and its initial curve can be expressed as follows:

$$u = \lambda\left[r\cos\vartheta + \frac{2z_0}{\lambda}\left(\frac{\partial w}{\partial r}\cos\vartheta - \frac{1}{r}\frac{\partial w}{\partial\vartheta}\sin\vartheta\right)\right],$$
$$v = \lambda\left[r\sin\vartheta + \frac{2z_0}{\lambda}\left(\frac{\partial w}{\partial r}\sin\vartheta + \frac{1}{r}\frac{\partial w}{\partial\vartheta}\cos\vartheta\right)\right], \tag{6}$$

and:

$$J' = r\begin{vmatrix} \cos\vartheta + \dfrac{2z_0}{\lambda}\left(\dfrac{\partial^2 w}{\partial r^2}\cos\vartheta + \dfrac{1}{r^2}\dfrac{\partial w}{\partial\vartheta}\sin\vartheta - \dfrac{1}{r}\dfrac{\partial^2 w}{\partial r\partial\vartheta}\sin\vartheta\right), & -\sin\vartheta + \dfrac{2z_0}{\lambda}\left(-\dfrac{\partial w}{\partial r}\sin\vartheta - \dfrac{1}{r}\dfrac{\partial w}{\partial\vartheta}\cos\vartheta + \dfrac{\partial^2 w}{\partial r\partial\vartheta}\cos\vartheta - \dfrac{1}{r}\dfrac{\partial^2 w}{\partial\vartheta^2}\sin\vartheta\right) \\ \sin\vartheta + \dfrac{2z_0}{\lambda}\left(\dfrac{\partial^2 w}{\partial r^2}\sin\vartheta - \dfrac{1}{r^2}\dfrac{\partial w}{\partial\vartheta}\cos\vartheta + \dfrac{1}{r}\dfrac{\partial^2 w}{\partial r\partial\vartheta}\cos\vartheta\right), & \cos\vartheta + \dfrac{2z_0}{\lambda}\left(\dfrac{\partial w}{\partial r}\cos\vartheta - \dfrac{1}{r}\dfrac{\partial w}{\partial\vartheta}\sin\vartheta + \dfrac{\partial^2 w}{\partial r\partial\vartheta}\sin\vartheta + \dfrac{1}{r}\dfrac{\partial^2 w}{\partial\vartheta^2}\cos\vartheta\right) \end{vmatrix} = 0. \tag{7}$$

Equations (6) can also be used for the determination of the pseudocaustic on the screen in the case when the coordinates (r, ϑ) of the points of the boundary of the plate are inserted in them.

3. CIRCULAR PLATES

(a) *Equations of caustics and pseudocaustics*

We consider now a simply supported circular plate of radius a loaded by a uniform load distribution q. The material of the plate is supposed to have a modulus of elasticity E and Poisson's ratio ν. Under these conditions, the expression for the deflection of the plate is [7, p. 57]:

$$w = \frac{q(a^2 - r^2)}{64D}(ka^2 - r^2), \quad k = \frac{5+\nu}{1+\nu}\left(0 \leqq \nu \leqq \frac{1}{2}, \frac{11}{3} \leqq k \leqq 5\right), \tag{8}$$

where D is the flexural rigidity of the plate.

Inserting relation (8) into eqns (6), we obtain:

$$u = \lambda r\cos\vartheta[1 - C(m - (r/a)^2)],$$
$$v = \lambda r\sin\vartheta[1 - C(m - (r/a)^2)], \tag{9}$$

where the constants C and m are defined by:

$$C = z_0 q a^2/(8\lambda D), \quad m = (k+1)/2 \quad (7/3 \leqq m \leqq 3). \tag{10}$$

The constant C will be supposed to be positive. This is a necessary, but not sufficient, condition so that a caustic exists, as it will be seen in the sequel.

If we consider on the screen a system of polar coordinates (ρ, φ), then eqns (9) result in:

$$\rho = \lambda r|1 - C(m - (r/a)^2)|, \quad \varphi = \vartheta \quad \text{or} \quad (\vartheta + \pi). \tag{11}$$

The pseudocaustic on the screen is obtained from eqns (11) by putting $r = a$. Thus, we obtain:

$$\rho_p = \lambda a|1 - C(m-1)|, \quad \varphi = \vartheta \quad \text{or} \quad (\vartheta + \pi), \tag{12}$$

that is the pseudocaustic is a circle of radius ρ_p lying on the screen.

The initial curve of the caustic on the plate is determined by considering eqn (5) and taking into account eqn (8). Thus, it is obtained:

$$J = [C(r/a)^2 - (Cm - 1)][3C(r/a)^2 - (Cm - 1)] = 0. \tag{13}$$

From eqn (13) there result two values of the radius r_i of the initial curve:

$$r_i = a(m - 1/C)^{1/2}, \tag{14a}$$

$$r_i = a((m - 1/C)/3)^{1/2}. \tag{14b}$$

The first of these values, because of eqn (11), gives on the screen $\rho = 0$. Hence, it cannot be considered as giving the radius of the initial curve of a caustic. On the contrary, the second of these values, under the assumption that:

$$Cm > 1, \tag{15}$$

constitutes the equation of the initial curve of the caustic on the plate. This curve has the shape of a circle.

By substituting this value of r_i into eqn (11), it is found that the caustic on the screen is also a circle of radius:

$$\rho_c = (2/3)\lambda a(3C)^{-1/2}(Cm - 1)^{3/2}. \tag{16}$$

It can also be remarked that the point of the caustic corresponding to the point (r, ϑ) of the initial curve has polar coordinates $(\rho_c, \vartheta + \pi)$, as it can be verified from eqns (9).

We can also remark that for a problem with radial symmetry eqn (7) for the initial curve of a caustic is simplified as:

$$\partial\rho/\partial r = 0. \tag{17}$$

By substituting the expression of ρ, given by eqn (11), into eqn (17), eqn (14b) of the radius r_i of the initial curve is obtained again.

(b) *Investigation of eqns* (14*b*) *and* (16)

As it was previously shown, the pseudocaustic forms the circumference of a circle of radius ρ_p given by eqn (12). It can be shown from eqn (12) that the pseudocaustic exists independently of the value of the constant C, which has been assumed to be positive. For $C = 0$, that is for an unloaded circular plate, there results $\rho_p = \lambda a$, which means that the circumference of the circle has been magnified on the screen with a magnification ratio equal to λ. As the constant C increases, the radius of the pseudocaustic decreases and for $C = 1/(m - 1)$ the pseudocaustic degenerates into the point $\rho = 0$. For a further increase of C, the radius ρ_p of the pseudocaustic begins to increase without limitations. These facts are shown in the following Table for the radius ρ_p of the pseudocaustic, considered as a function of C:

C	0	increases	$1/(m-1)$	increases
ρ_p	λa	decreases	0	increases

An analogous investigation can be also made for the radius of the caustic on the screen. As it was previously pointed out, a caustic is formed on the screen only if inequality (15) is satisfied. In this case, the radius ρ_c of the caustic is given by eqn (16). From this equation we observe that, because of limitation (15), the term $(Cm - 1)$ is always positive. Because of the relation: $7/3 \leqq m \leqq 3$, it can be concluded that the initial curve of the caustic on the plate, the radius r_i of which is given by eqn (14b), lies always inside the circular plate, tending to coincide with its circumference when the constant C tends to infinity and at the same time Poisson's ratio ν of the material of the plate tends to zero, since in this case $k \to 5$ and $m \to 3$. Hence, under the limitation (15), there is always an initial curve on the plate and a caustic on the screen.

As regards the radius ρ_c of the caustic, given by eqn (16), the limitation (15) being satisfied, it increases as the value of the constant C increases. These facts are shown in the following table for the radius ρ_c of the caustic, considered as a function of C:

C	0 increases	$1/m$	increases
ρ_c	there is no caustic	0	increases

Since the radius ρ_p of the pseudocaustic decreases as C increases up to the value $1/(m-1)$ (in which case $\rho_p = 0$), whereas the radius ρ_c of the caustic increases as C increases from the value $1/m$ (in which case $\rho_c = 0$), there follows that for a value of C in the interval:

$$1/m < C < 1/(m-1) \tag{18}$$

the pseudocaustic and the caustic will have equal radii ($\rho_p = \rho_c$) and, therefore, they will coincide on the screen. This value of C, resulting by equating the radii ρ_p and ρ_c of the pseudocaustic and the caustic, given by eqns (12) and (16) respectively, will be a root of the following equation of the third degree:

$$[4m^3 - 27(m-1)^2]C^3 - 6[2m^2 - 9(m-1)]C^2 + 3[4m - 9]C - 4 = 0. \tag{19}$$

For the special case where $m = 3$, there results $C = 4/9$, a value which is in agreement with the limitation (18). Furthermore, it can be easily seen that the sum of the roots of eqn (19) is negative, while their product is positive. Since this equation is of the third degree and has, as it was already mentioned, one positive root, it follows that its other two roots are either negative or complex. But in both these cases these roots are of no importance. It can also be noted that, the constant C tending to infinity, the caustic remains lying outside the pseudocaustic. It can be finally remarked that the points of the screen constituting the image of the plate are the points of the circle defined by the pseudocaustic or the caustic, this depending on which of these two curves has the greater radius, since it is impossible that the image of the plate on the screen has the form of an annulus.

Extensive experimental evidence was provided for the above-established theoretical results. Thin circular plates of radius $a = 4.1$ cm were cut from a plain plexiglas sheet of thickness $t = 0.21$ cm. The elastic modulus and Poisson's ratio of plexiglas were determined by a tension specimen and found to be $E = 32{,}000\ \mathrm{kp/cm^2}$ and $\nu = 0.36$. From these values the flexural rigidity D of the plate, given by the relation[7, p. 5]:

$$D = \frac{Et^3}{12(1-\nu^2)}, \tag{20}$$

was calculated and found to be $D = 28.37$ kp cm. The plexiglas plates were put to a simple jig for the application of the load.

For obtaining the caustics and pseudocaustics of the loaded plates a He–Ne laser light beam was impinged on the specimens and the reflected light rays were received on a reference screen. A schematic diagram of the experimental apparatus is shown in Fig. 2.

In order to get a series of caustics corresponding to various values of the global constant C and thus to verify the above-established theoretical considerations, the reference screen was placed at various distances z_0 from the specimen. To each such position the values of the constant C were determined from the first of eqns (10) with the value of the magnification ratio λ being equal to 1. Moreover, from the second of eqns (8) and (10) it was found that $k = 3.94$ and $m = 2.47$, while the loading intensity q was equal to $q = 0.245\ \mathrm{kp/cm^2}$. As regards the distance between the specimen and the screen, it was variable.

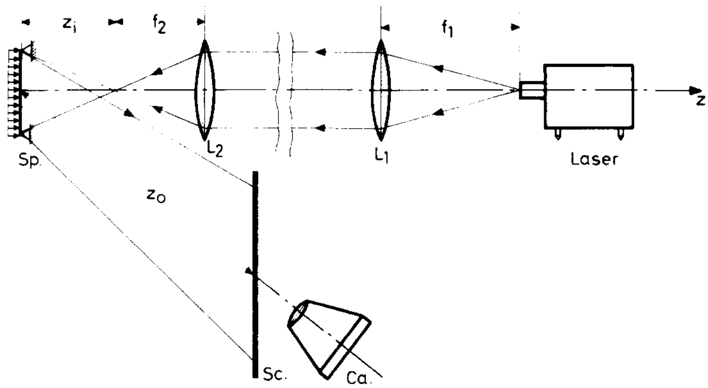

Fig. 2. Schematic diagram of the experimental apparatus.

Figure 3 presents a series of six optical patterns obtained on the screen by moving progressively it with respect to the specimen. These patterns corresponded to the following values of the constant C: $C = 0.362$ (a), 0.507 (b), 0.598 (c), 0.725 (d), 0.761 (e) and 1.160 (f). It can be observed from Fig. 3a that the only curve that is formed on the reference screen is the pseudocaustic and that no caustic is formed. This corroborates the previously established result that, when $C < 1/m$, no caustic is formed. Indeed, for the Fig. 3(a) this relation is satisfied ($C = 0.362$, $1/m = 0.405$). Nevertheless, even in Fig. 3(a), a highly illuminated region around the centre of the image of the plate on the screen is observed. This fact denotes that the caustic is about to be formed after a small increase of C. In Fig. 3(b) a small caustic is seen and the radius ρ_p of the pseudocaustic decreased, compared to its value corresponding to Fig. 3(a) ($1/m < C < C_0$ where C_0 corresponds to the case where $\rho_p = \rho_c$; the value of C_0 was calculated from eqn (19) and it was found to be $C_0 = 0.581$). In Fig. 3(c) the radii of the pseudocaustic ρ_p and the caustic ρ_c are almost equal ($C \simeq C_0 = 0.581$). In Fig. 3(d) the radius of the pseudocaustic ρ_p is almost zero while the radius of the caustic ρ_c is always increasing ($C \simeq 1/(m-1) = 0.680$). In Fig. 3(e) the radius of the pseudocaustic ρ_p begins to increase again like the radius of the caustic ρ_c ($C > 1/(m-1) = 0.680$). The region of the screen corresponding to the whole plate is

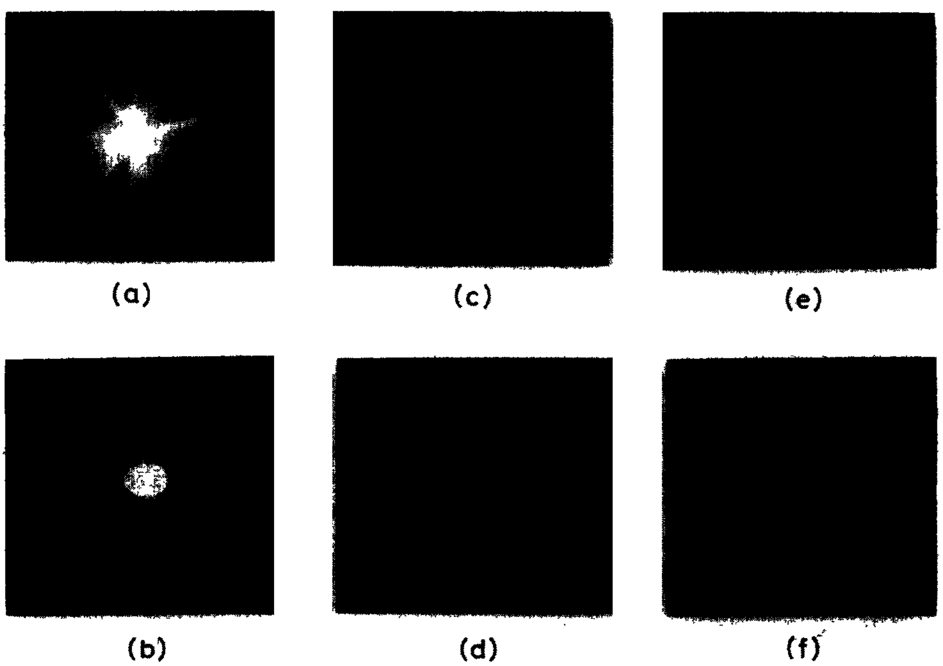

Fig. 3. Experimentally obtained pseudocaustics and caustics for a simply supported and uniformly loaded circular plate.

included inside the caustic, the circle defined by the pseudocaustic included also in it. Each point inside the pseudocaustic ($\rho < \rho_p$) on the screen corresponds only to one point of the plate, while each point inside the annulus ($\rho_p < \rho < \rho_c$) corresponds to two completely different points of the plate, of course lying on the same polar direction. Finally, in Fig. 2(f) it is seen that the radius of the pseudocaustic ρ_p remains smaller than the radius of the caustic ρ_c as it was already concluded theoretically.

For all the optical patterns pictured in Fig. 3 the corresponding radii ρ_c and ρ_p of the caustics and the pseudocaustics were calculated through eqns (16) and (12) respectively from the values of the constants a, λ, C and m. Thus, a quantitative comparison with the caustics of Fig. 3 was made. It was found that the radii ρ_c and ρ_p should take the following values in cm, corresponding to the photographs of Fig. 3: $\rho_c = 0.283$ (b), 0.674 (c), 1.305 (d), 1.495 (e) and 3.735 (f) and $\rho_p = 1.914$ (a), 1.040 (b), 0.493 (c), 0.272 (d), 0.490 (e) and 2.895 (f). By comparing these values of the radii ρ_c and ρ_p with the corresponding experimental values, it was seen that the divergence between these two sets of values was in all cases less than 0.2 cm. This small divergence between the theoretical and experimental results proves the potentiality of the technique developed for the solution of flexed plate problems.

4. EQUILATERAL TRIANGULAR PLATES

We consider now an equilateral triangular plate of height a referred to a coordinate system Oxy with centre O coinciding with the centre of the triangle and its Ox-axis along a height of the triangle (Fig. 4). If this plate is considered simply supported and loaded by a uniform load q, the following relation determines the deflection $w(x, y)$ of its points $P(x, y)$ [7, p. 313]:

$$w = \frac{q}{64aD}[x^3 - 3y^2x - a(x^2+y^2) + 4a^3/27](4a^2/9 - x^2 - y^2), \tag{21}$$

where D is again the flexural rigidity of the plate.

By substituting this value of w into eqn (5), we obtain, after some algebra, for the initial curve of the caustic:

$$(1 + CA)^2 = (C^2/a^6)(B^2 + E^2), \tag{22}$$

where

$$A = (2/a^3)[-x^3 + 3xy^2 + a(x^2+y^2) - 4a^3/27], \tag{23}$$

$$B = -3x^3 - 3xy^2 + a(x^2 - y^2) + 2a^2x/3,$$
$$E = (3x^2 + 3y^2 + 2ax - 2a^2/3)y. \tag{24}$$

Equation (22) for the initial curve of the caustic can be written in polar coordinates as:

$$[1 - 2(C/a^3)(r^3\cos 3\vartheta - ar^2 + 4a^3/27)]^2$$
$$= (C^2/a^6)[(3r^2 - 2a^2/3)^2r^2 + a^2r^4 - 2a(3r^2 - 2a^2/3)r^3\cos 3\vartheta]. \tag{25}$$

From eqn (25) we observe that, if we replace ϑ by $(-\vartheta)$ or $(\vartheta \pm 2\pi/3)$, this equation does not change, as it was expected because of the symmetry of the triangular plate. Consequently, it is sufficient to solve eqn (25) with respect to r only in the interval $0 \leqq \vartheta \leqq \pi/3$. The corresponding points of the caustic on the screen can be afterwards easily found by using eqns (2).

These equations can be also used for the determination of the point $P'(u, v)$ of the screen corresponding to any point $P(x, y)$ of the plate. In particular, the edges of the triangular plate will give the points of the pseudocaustic on the screen. Because of the symmetry of triangular plate, it is sufficient to consider only one of its edges, e.g.: $x = -a/3$, $-a/\surd(3) \leqq y \leqq a/\surd(3)$, and to determine the corresponding side of the pseudocaustic on the screen. Thus, from eqn (21) we find for the points of the edge of the plate considered:

$$\frac{\partial w}{\partial x} = \frac{q}{64aD}(3y^4 - 2a^2y^2 + a^4/3), \quad \frac{\partial w}{\partial y} = 0. \tag{26}$$

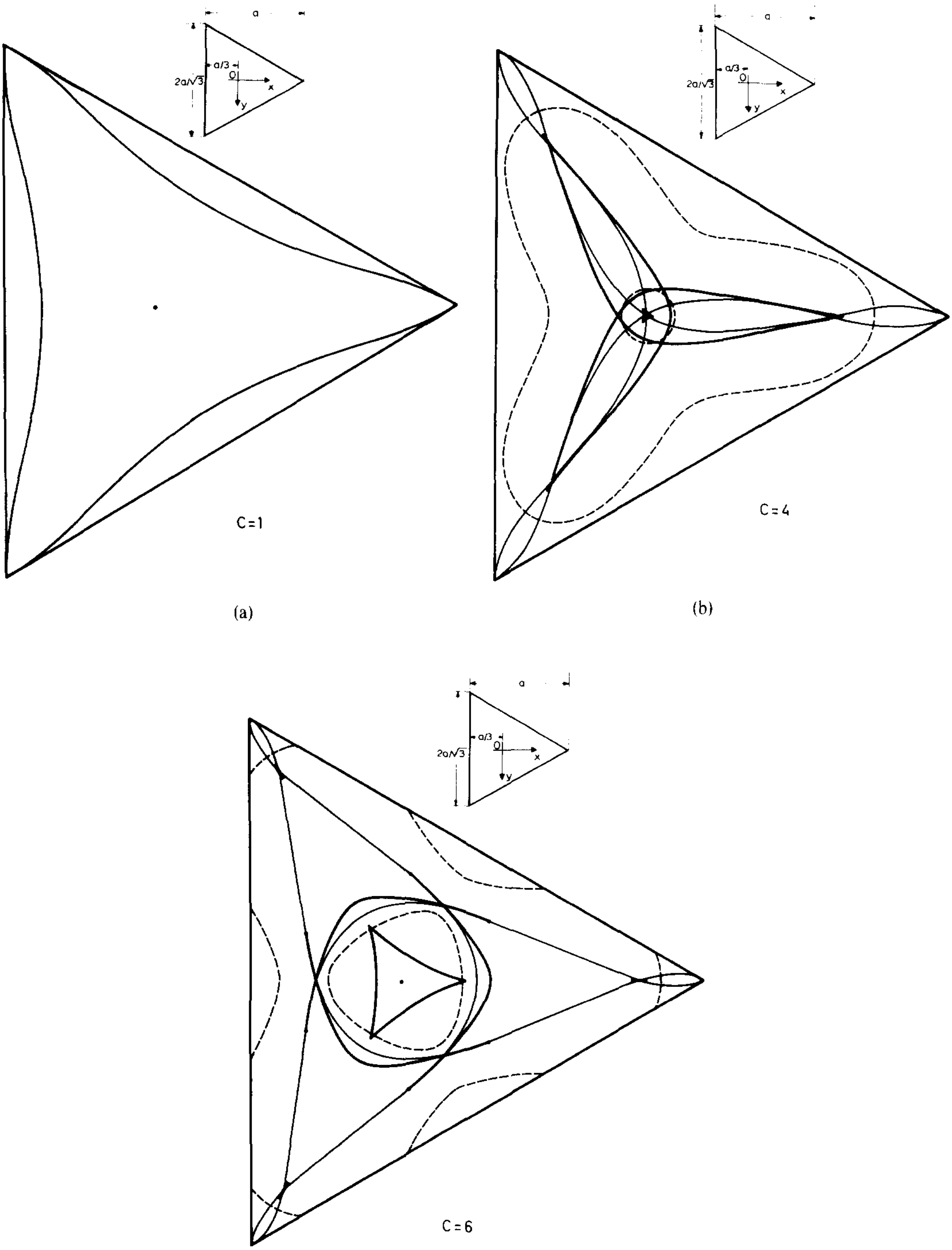

Fig. 4. Theoretically obtained pseudocaustics (——), initial curves (------) and caustics (———) for a simply supported and uniformly loaded equilateral triangular plate ($\lambda = 1$).

The second of these equations is obvious because the triangular plate is simply supported along its edges. Then eqns (2) give for the points $P'(u_p, v_p)$ of the corresponding side of the pseudocaustic:

$$u_p = \lambda[-a/3 + C(3y^4 - 2a^2y^2 + a^4/3)/(4a^3)], \quad v_p = \lambda y,$$
$$-a/\sqrt{(3)} \leqq y \leqq a/\sqrt{(3)}, \tag{27}$$

the constant C given again by the first of eqns (10).

In accordance with these developments, the pseudocaustics, initial curves and caustics corresponding to the cases $C = 1$, $C = 4$ and $C = 6$ have been determined and are shown in Figs. 4(a)–4(c) respectively. It can be noted that for small values of C (as in Fig. 4(a)) no caustic exists. In Figs. 5(a)–5(c) the experimentally obtained pseudocaustics and caustics, corresponding to those shown in Figs. 4(a)–4(c) respectively, are presented. The experimentally obtained caustics of Figs. 5(a)–5(c) are satisfactorily compared with their corresponding theoretical forms of Figs. 4(a)–4(c).

Finally, we can remark that, although the form of the caustic completely changes as the loading intensity q (and the constant C because of the first of eqns (10)) increases, nevertheless, the shape of pseudocaustics does not change too much as it can also be seen from eqns (27) for increasing values of C, which almost plays the role of a magnification ratio.

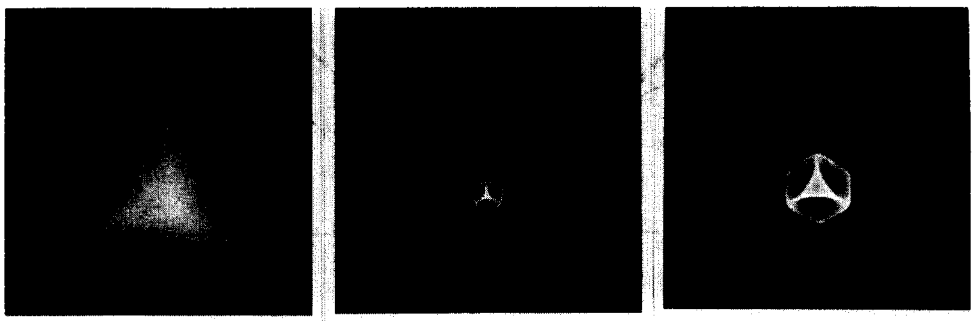

(a) (b) (c)

Fig. 5. Experimentally obtained pseudocaustics and caustics for a simply supported and uniformly loaded equilateral triangular plate.

5. SQUARE PLATES

As a last example we consider a simply supported square plate of side a loaded by a uniform load q. A coordinate system Oxy with its centre O at the middle of one side of the square and its Oy-axis coinciding with this side is attached to the plate (Fig. 6). The deflection $w(x, y)$ of the points $P(x, y)$ of the plate is given by [7, p. 115]:

$$w = \frac{q}{24D}(x^4 - 2ax^3 + a^3x) + \frac{qa^4}{D}\sum_{m=1,3,5,\dots}^{\infty}\left(A_m \cosh\frac{m\pi y}{a} + B_m \frac{m\pi y}{a}\sinh\frac{m\pi y}{a}\right)\sin\frac{m\pi x}{a}, \tag{28}$$

where D denotes again the flexural rigidity of the plate and the coefficients A_m and B_m are determined by:

$$A_m = -\frac{2(c_m \tanh c_m + 2)}{\pi^5 m^5 \cosh c_m}, \quad B_m = \frac{2}{\pi^5 m^5 \cosh c_m}, \quad c_m = \frac{m\pi}{2}. \tag{29}$$

The equations of the initial curve of the caustic and the caustic can be determined by substituting the derivatives of $w(x, y)$ with respect to x and y in eqns (2) and (5).

We can also determine the part of the pseudocaustic formed on the screen from an edge of the plate. If we consider, for example, the edge: $x = 0$, $-a/2 \leqq y \leqq a/2$ of the square plate, we find for its points from eqn (28):

$$\frac{\partial w}{\partial x} = \frac{qa^3}{D}\left[\frac{1}{24} + \sum_{m=1,3,5\dots}^{\infty} m\pi\left(A_m \cosh\frac{m\pi y}{a} + B_m \frac{m\pi y}{a}\sinh\frac{m\pi y}{a}\right)\right], \quad \frac{\partial w}{\partial y} = 0, \tag{30}$$

the second of these equations justified by the fact that the square plate was considered simply supported. Then, eqns (2) give for the points $P'(u_p, v_p)$ of the corresponding side of the pseudocaustic:

$$u_p = -(\lambda - 1)a/2 + 2z_0\partial w/\partial x, \quad v_p = \lambda y \quad (x = 0, -a/2 \leqq y \leqq a/2), \tag{31}$$

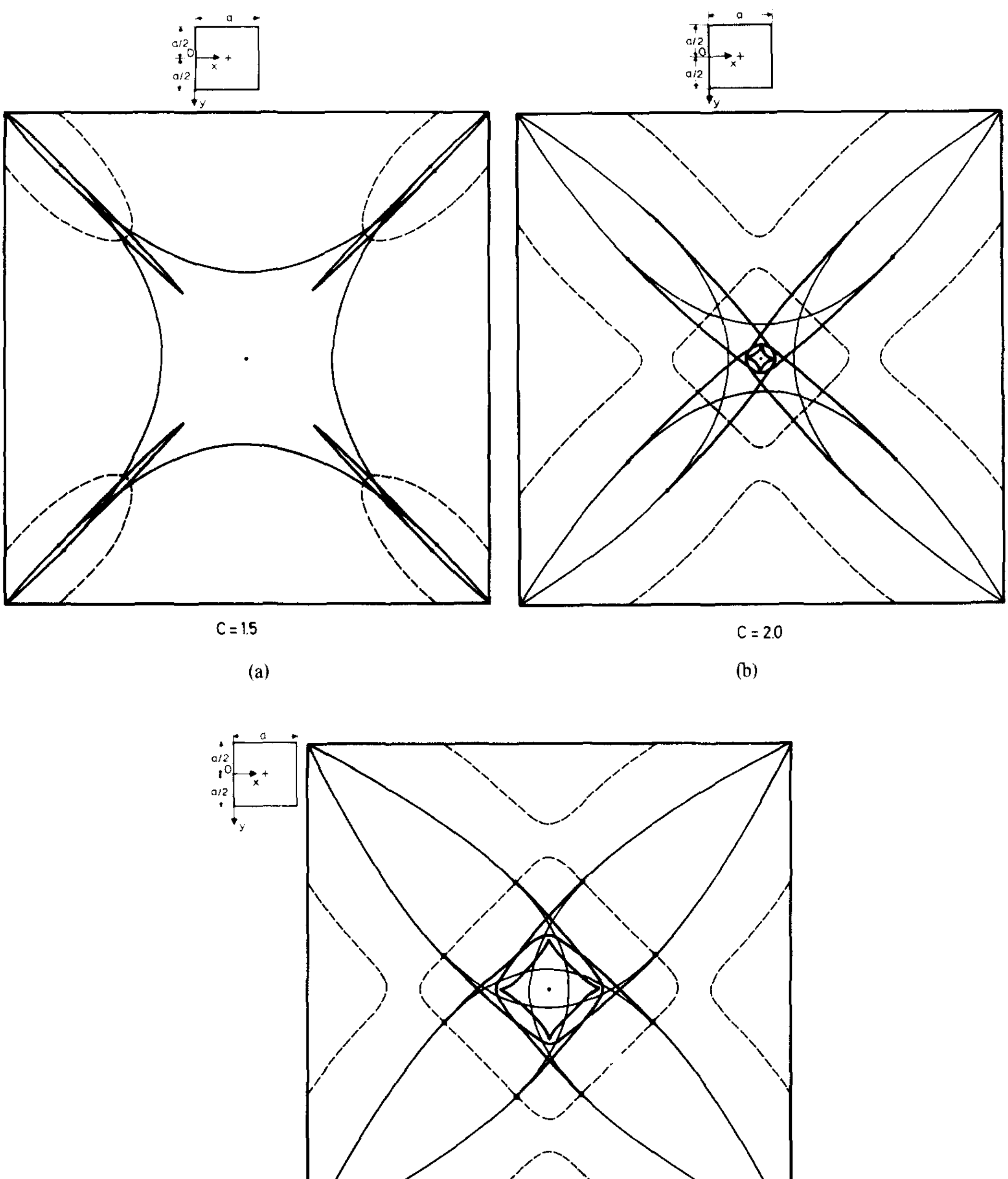

Fig. 6. Theoretically obtained pseudocaustics (——), initial curves (-----) and caustics (——) for a simply supported and uniformly loaded square plate (λ = 1).

where $\partial w/\partial x$ for $x = 0$ is given by the first of eqns (30). Also the light beam has been considered incident normally at the centre of the square plate and not at the origin O of the coordinate system. Because of the symmetry of the square plate and the way of its loading, it is sufficient for determining the whole pseudocaustic, that only one of its sides be determined through eqns (30) and (31).

In accordance with these considerations, the pseudocaustics, initial curves and caustics, corresponding to the cases where the constant C, given by the first of eqns (10), is equal to 1.5, 2.0 2.5, have been determined and shown in Figs. 6(a)–6(c) respectively. Furthermore, in Figs. 7(a)–7(c) the experimentally obtained pseudocaustics and caustics, corresponding to those shown in Figs. 6(a)–6(c), are shown. The coincidence of the theoretically and experimentally obtained

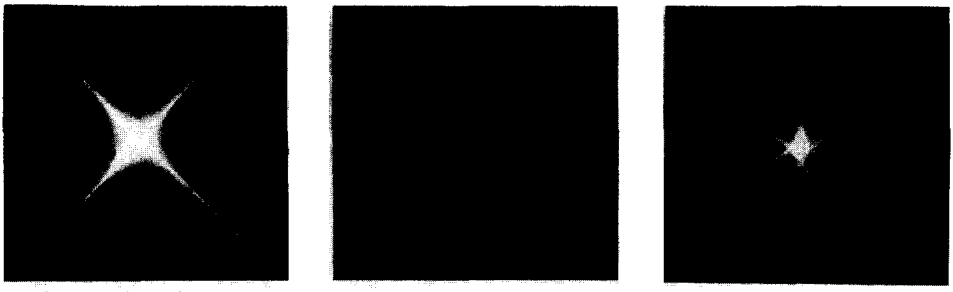

(a) (b) (c)

Fig. 7. Experimentally obtained pseudocaustics and caustics for a simply supported and uniformly loaded square plate.

pseudocaustics and caustics is again excellent, as in the cases of circular and equilateral triangular plates.

Finally, for increasing values of the loading intensity q, it is observed that the shape of the caustics changes significantly although the same is not true for the shape of pseudocaustics, exactly as happened in the case of an equilateral triangular plate.

CONCLUSIONS

In this paper the method of caustics, already successfully used for the solution of a large number of singular elastic and plastic stress fields, was applied to the case of simply supported and uniformly loaded plates. It was shown that the pseudocaustics and caustics, created by the boundaries of the plates and the initial curves respectively, can be easily determined both theoretically and experimentally. For the cases of a circular, an equilateral triangular and a square plate considered in detail, the theoretically and experimentally obtained pseudocaustics and caustics are in very good agreement. This fact, together with the theory developed in this paper, can be used for the experimental evaluation of the existing loading of the plate by simple measurements of some geometrical characteristics of the pseudocaustics and caustics created.

Acknowledgements—The author is indebted to his assistant Dr. Nick Ioakimidis for carrying out all the calculations contained in the paper and to his technician Mr. A. Koutsambessis for executing the experiments included in this investigation. The research work contained in the paper is partly supported by a University fund.

REFERENCES

1. P. S. Theocaris, Local yielding around a crack-tip in plexiglas. *J. Appl. Mech.* **37**, 409 (1970).
2. P. S. Theocaris, Complex stress intensity factors at bifurcated cracks. *J. Mech. Phys. Solids* **20**, 265 (1972).
3. P. S. Theocaris, Stress singularities at concentrated loads. *Exp. Mech.* **13**, 511 (1973).
4. P. S. Theocaris and E. E. Gdoutos, The modified Dugdale–Barenblatt model adapted to various fracture configurations in metals. *Int. J. Fract.* **10**, 549 (1974).
5. P. S. Theocaris, Stress and displacement singularities near corners. *Zeit. ang. Math. Phys.* **26**, 77 (1975).
6. P. S. Theocaris and E. E. Gdoutos, Experimental solution of flexed plates by the method of caustics. *J. Appl. Mech.* **44**, 107 (1977).
7. S. P. Timoshenko and S. Woinowsky-Krieger, *Theory of Plates and Shells*. 2nd Edn. McGraw-Hill, New York (1959).